Applied Mathematical Modelling 89 (2021) 627–635

Contents lists available at ScienceDirect

Applied Mathematical Modelling

journal homepage: www.elsevier.com/locate/apm

Synchronization of energy transmission networks at low voltage levels

Juliana C. Lacerda [a,*], Jussara Dias [a], Celso Freitas [a], Elbert Macau [b]

[a] Associated Laboratory for Computing and Applied Mathematics, National Institute for Space Research, INPE, São José dos Campos, SP 12243-010, Brazil

[b] Institute of Science and Technology, Federal University of São Paulo, São José dos Campos, SP 12247-014, Brazil

ARTICLE INFO

Article history:
Received 29 April 2020
Revised 24 June 2020
Accepted 12 July 2020
Available online 6 August 2020

Keywords:
Power grid
Synchronization
Kuramoto model

ABSTRACT

Power grids or energy transmission networks are among the biggest and more complex man made constructions ever made and are a typical example of a complex system. Its components need to be in a synchronous state in order to be fully functional and avoid cascade failures and blackouts. Power grids can be modeled as a complex network of oscillators, where each node represents a generator or a consumer and the transmission lines are represented by edges. In this work, we show how to build a power grid topology that presents relatively low number of edges and favors synchronization as a low value of coupling is required to reach the synchronous state. As the coupling is related to the maximum transmission capacity of a transmission line, lower coupling in this context means lower voltage levels. The basin stability of this network is also calculated as it appears to have a higher quantity of stable nodes when compared to a random network. The methodology presented in this work is based on an evolutionary optimization framework and would be of great interest when building power grids due to the costs involved in the construction of transmission lines, as there would be less lines and they would be required to operate in a lower voltage level.

1. Introduction

Power transmission systems are crucial to economic prosperity worldwide as interruptions in the transmission and generation in electricity networks can cause economic and social problems for the whole society [1]. Power grids are naturally complex as they are one of the biggest constructions ever made, and, in order to be fully functional, all of its components must be in a synchronous state and they must be robust enough to go back to this state even when subjected to failures and disturbances [2], which represents an enormous challenge for stability analysis. Therefore, engineers and researchers must be able to accurately analyze the stability of power systems taking into consideration scenarios that can cause disturbances in the network implying local failures and in some cases, blackouts of high proportions [3].

Instabilities in power grids can be caused, for example, by the malfunctioning of some of its components, due to climatic factors such as fire, rain and lightning [4,5] or if a renewable source of energy becomes unavailable [6] due to its proper characteristics. Interruptions in energy transmission duo to climatic problems have a great impact on the network infrastructure, being considered one of the main causes of problems in power grids world wide [5]. The growing integration of

* Corresponding author.
E-mail addresses: juliana.lacerda@inpe.br (J.C. Lacerda), elbert.macau@unifesp.br (E. Macau).

https://doi.org/10.1016/j.apm.2020.07.049
0307-904X/

renewable energy sources in transmission networks is stimulated by environmental and economic issues. Microgrid is one of the technologies that can integrate large amounts of renewable energy such as solar, wind and geothermal systems, and fulfills the distributed generation potential of a system [7]. However, the generation of renewable energy is intermittent, stochastic and subject to climatic conditions, so it can cause unforeseen fluctuations in the system and is one of the major causes of instability in transmission networks today [8].

A way to properly study power grids is by using the concepts of complex networks. In this representation, the transmission lines are modeled by edges and the generators and consumers are represented by nodes. The second order Kuramoto model is often applied in frequency synchronization problems, for example, in networks of electric power transmission [9] and forced pendulum dynamics [10] and is used in this work to describe the dynamics of generators and consumers. In this model, the coupling constant relates to the maximum power transmission capacity of the transmission lines, while the phase and the angular velocity evolve as time passes and the synchronization is damped by a term of inertia [11].

By using the second order Kuramoto model to study power grids, a model of basin stability in relation to strong perturbations was proposed in order to study the stability of electric networks that also may be applied to other dynamical systems [12]. It was shown that there are some patterns called dead ends and dead trees in power grids that reduce the overall dynamic stability of the system [13].

The evolutionary optimization technique called evolutionary edge-snapping [14,15] is used in this work to generate a network topology that favors synchronization for rather small values of coupling. This method creates networks with a relatively small number of edges and these topologies would be of great interest in designing of power grids, due to the costs involved in the construction of transmission lines. Further, as the system enters the synchronous state at a low coupling (compared to the coupling obtained when studying a random network with the same number of nodes and edges), it means that lower voltage levels are needed in the transmission lines [16,17], which is also a desirable characteristics. After studying and analyzing the behavior of the power grid topology created by the Edge Snapping method, we use the one-node basin stability method [13] to analyze the stability of this topology when subjected to large perturbations. We find that this network appears to have a higher number of stable nodes when compared to a random network.

2. Model and methods

In this section, we present the model used to describe the dynamics of the components (generator and consumers) of a power grid, metrics to quantify the level of synchronization of this system, both in Section 2.1, and a model to generate topologies of power grids in Section 2.2. In Section 2.3, a method to study the stability of the components of this power grid is presented.

2.1. Synchronization metrics and second order Kuramoto model

In order for a power grid to be fully functional, all of its components must be frequency synchronized [2]. So we begin this section by presenting metrics that quantify the level of synchronization of a dynamical system. The *order parameter* $R(t)$ [18] shows the level of the collective behavior of a system by measuring the amount of phase synchronization. It is defined as

$$R(t) = \left| \frac{1}{N} \sum_{m=1}^{N} e^{i\theta_m(t)} \right|, \tag{1}$$

where i is the imaginary unit, $\theta(t)$ is the phase of oscillator m and N is the total number of nodes. $R(t) \in [0, 1]$, in a way that when all oscillators have the same phase, that is, when the system presents phase synchronization, $R(t) = 1$. The mean over time of the order parameter $R(t)$ will be called R.

The parameter *partial synchronization index* [19] presents the level of the frequency synchronization (or phase locking) [20,21] between a pair of a system' units and is given by

$$S_{mn} = \left| \lim_{\Delta t \to \infty} \frac{1}{\Delta t} \int_{t_r}^{t_r + \Delta t} e^{i[\theta_m(t) - \theta_n(t)]} dt \right|, \tag{2}$$

where m and n are the label of the nodes and t_r is a transient time. In order to measure the level of frequency synchronization of the whole network, we calculate the arithmetic mean

$$S = \frac{1}{N^2} \sum_{m,n=1}^{N} S_{mn}. \tag{3}$$

$S \in [0, 1]$ and when $S = 1$, the system is phase locked, meaning that the phase difference between all pair of nodes is constant through time, thus having the same instantaneous frequency.

In order for power to flow in a power grid, there must be a phase difference between the components of the grid [11]. So, we want our system to be phase locked, thus having the same instantaneous frequency, and not phase synchronized, that is, we want $S = 1$ and $R \neq 1$, and we will be referring to this configuration when we say that the system is synchronized.

In order to model the dynamics of generators and consumers, we make use of the second order Kuramoto model [22] in a way that the dynamics of a power grid component m is given by:

$$\ddot{\theta}_m = -\alpha\dot{\theta}_m + \omega_m + \frac{\lambda}{g_m}\sum_{n=1}^{N} A_{mn}\sin(\theta_n - \theta_m), \tag{4}$$

for $m = 1, \ldots, N$, $\alpha \in \mathbb{R}$ is the dissipation parameter ($\alpha = 0.1$ is used in this work), λ is the coupling constant and it represents the maximum power transmission capacity of the transmission line that connects the nodes in a power grid (note that λ is the same for our entire network), ω_m is the natural frequency of oscillator m and here it represents the amount of power delivered by ($\omega_m > 0$, generator) or consumed by ($\omega_m < 0$, consumer) node m, g_m and θ_m are the degree and phase of oscillator m, respectively. The degree g of a node m represents the number of edges that are incident to this node. A_{mn} are the entries of the adjacency matrix, being equal to 1 if oscillators m and n are connected (there is a transmission line between them) and 0 otherwise. Eq. (4) can be also written as:

$$\dot{\theta}_m = \nu_m, \tag{5}$$

$$\dot{\nu}_m = -\alpha\nu_m + \omega_m + \frac{\lambda}{g_m}\sum_{j=1}^{N} A_{mn}\sin(\theta_n - \theta_m), \tag{6}$$

where ν_m is the angular velocity (instantaneous frequency) of node m.

The phase and the angular velocity of a node m in the synchronous state are defined as (θ_m^S, ν_m^S). The phase in the synchronous state is [13,23]

$$\theta_m^S = \arcsin\frac{\omega_m}{\lambda}, \tag{7}$$

and the synchronous angular velocity is given by [9,11]

$$\nu_m^S = \sum_{m=1}^{N}\frac{\omega_m}{N\alpha}. \tag{8}$$

In this work, there are $\frac{N}{2}$ consumers ($\omega_m < 0$) and $\frac{N}{2}$ generators ($\omega_m > 0$) in a way that all power generated is consumed, so $\sum_{m=1}^{N}\omega_m = 0$ and, therefore, $\nu_m^S = \nu^S = 0$.

2.2. Edge snapping method

The *edge snapping method* [14,24] is used in this work in order to generate topologies that model a power grid. This method is an adaptive strategy that drives the evolution of an unweighted network, in which a second order equation is associated with each edge of the graph. It has been chosen because it generates networks with a relatively low number of edges (transmission lines) [24] and, as will be presented in Section 3, it allows the network to be synchronized at lower values of coupling, thus requiring transmission lines with lower maximum transmission capacity, which, along with the lower number of transmission lines, would be economically desirable.

The equation associated with the edge between nodes m and n is given by

$$\ddot{k}_{mn} + d\dot{k}_{mn} + \frac{\partial V(k_{mn})}{\partial k_{mn}} = h(||\theta_m - \theta_n||), \tag{9}$$

where $d = 1$ is a constant damping factor, h is an external force and k_{mn} is the coupling gain. $V(k_{mn})$ is a double-well potential given by

$$V(k_{mn}) = bk_{mn}^2(k_{mn} - 1)^2, \tag{10}$$

in which $b = 1$ is a constant. $V(k_{mn})$ has two local minima, $k_{mn} = 0$ and $k_{mn} = 1$, in a way that if $k_{mn} = 1$ we define that there is an edge between nodes m and n and if $k_{mn} = 0$ there is not. At the beginning of evolution of Eq. (9), all nodes are disconnected and the initial conditions are $k_{mn}(0) = 0$ and $\dot{k}_{mn}(0) = 0$. Due to the external force h, k_{mn} may come out of its initial equilibrium point $k_{mn} = 0$ (edge is not present) and move to the other local minima $k_{mn} = 1$ (edge is present). The external force in this work is defined as $h(||\theta_m - \theta_n||) = 1 - |\theta(m) - \theta(n)|$.

By using the edge snapping method to generate network topologies, the second order Kuramoto model is written as

$$\ddot{\theta}_m = -\alpha\dot{\theta}_m + \omega_m + \frac{\lambda}{g_m}\sum_{n=1}^{N} k_{mn}\sin(\theta_n - \theta_m). \tag{11}$$

Note that the only difference between Eqs. (4) and (11) is that in the latter the adjacency matrix A is replaced by the coupling gain k given by Eq. (9). So, in order to study the dynamics of our power grid, we integrate Eqs. (9) and (11) simultaneously.

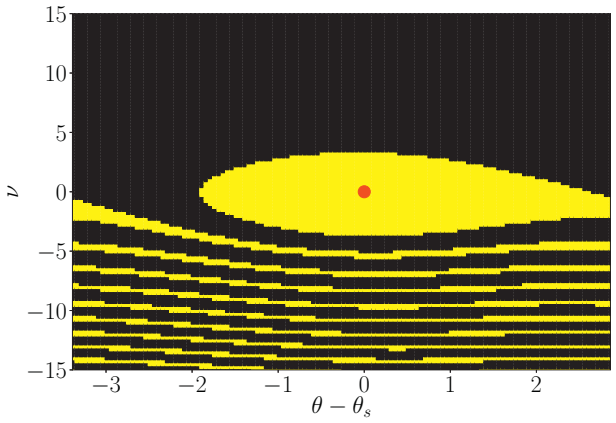

Fig. 1. Basin of attraction (yellow) of a single node dynamics given by Eq. (13). The synchronous state $(\theta_m^S, 0)$ is plotted as a red dot. (For interpretation of the references to color in this figure legend, the reader is referred to the web version of this article.)

2.2.1. Evolutionary edge snapping

The edge snapping method is used in the context of evolutionary optimization where rules of variation and selection are applied in order to generate network topologies. The evolutionary edge snapping is composed of two fundamental rules [15,24]:

Rule 1 – Variation: A set of $n_T = 100$ network topologies is generated by integrating Eqs. (9) and (11), with Eq. (11) staring from n_T distinct initial conditions that are randomly generated by a uniform distribution between $[0, 2\pi)$. From this set of n_T topologies, we calculate the fraction between the number of networks where the edge between the nodes m and n is present (n_{mn}) and the total number of topologies that were generated. This fraction is the probability of activation of the edge between nodes m and n

$$F_{mn} = \frac{n_{mn}}{n_T}, \tag{12}$$

where $0 \leq F_{mn} \leq 1$.

Rule 2 – Selection: Only edges with activation probability F_{mn} higher than a certain threshold f^* are marked as active (are present) in the network. The value of f^* is chosen in a way that the entire network is connected and present the smallest possible number of edges, we call this network *minimal edge-snappping network (ES network).*

2.3. Basin stability

A basin of attraction B is the set of initial conditions that, as the system evolves in time, tends to an attracting fixed point [10]. In order to visualize the basin of attraction of a node m in a power grid, consider a single node dynamics given by

$$\begin{aligned} \dot{\theta}_m &= \nu_m, \\ \dot{\nu}_m &= -\alpha\nu_m + \omega_m + \lambda \sin(\theta_{grid} - \theta_m), \end{aligned} \tag{13}$$

where $\theta_{grid} = 0$, as we consider that the rest of the network is not affected by node m. In order to find the basin of attraction, we integrate Eq. (13) fixing $\lambda = 4.0$ and $\omega = 1.0$ for distinct values of initial conditions $(\theta(0), \nu(0))$, where $\theta \in [0, 2\pi]$ and $\nu \in [-15, 15]$ and annotate for which conditions the system evolved to the synchronous state $(\theta_m^S, \nu^S = 0)$. This basin of attraction can be seen in Fig. 1, it is colored in yellow and the red dot represents the attracting fixed point describing the synchronous state.

Looking from another perspective, we can assume that at a time t_1, node m is at the synchronous state $(\theta_m(t_1), \nu_m(t_1)) = (\theta_m^S, 0)$ and suffers a perturbation at time t_2 in a way that $(\theta_m(t_2), \nu_m(t_2)) \neq (\theta_m^S, 0)$. So, if $(\theta_m(t_2), \nu_m(t_2))$ is outside of the basin of attraction, the node will not go back to the synchronous state, and, on the other hand, if $(\theta_m(t_2), \nu_m(t_2))$ is inside the basin of attraction, the dynamics of the node will reach the synchronous state after a certain amount of time.

The single-node basin stability method [13] is applied in study of the stability of the second order Kuramoto network generated by the Edge Snapping method. The basin stability E of a node m is defined as

$$E_m = E(B_m) = \int \chi_B(\theta, \nu)\rho(\theta, \nu)d\theta d\nu, \tag{14}$$

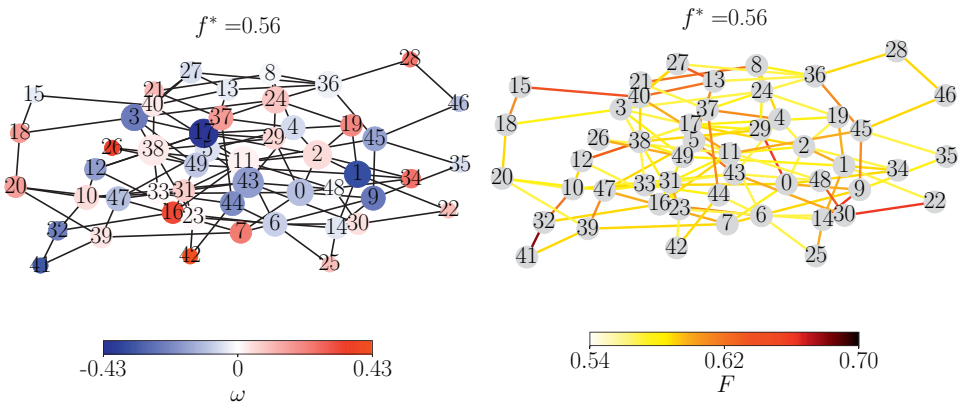

Fig. 2. 50 node ES network with threshold $f^* = 0.56$ and 108 edges. (a) The size of the nodes is proportional to their degree and their color relates to the consumed (blue) or delivered (red) power ω. (b) Probability of activation F of the edges. (For interpretation of the references to color in this figure legend, the reader is referred to the web version of this article.)

where ρ is a probability density ($\int \rho(\theta, \nu) d\theta d\nu = 1$) related to the states that the system can reach due to perturbations and in order to perform our calculations, ρ is defined as

$$\rho = \begin{cases} \dfrac{1}{|Q|}, & \text{if } (\theta, \nu) \in Q, \text{where } \; Q = [0, 2\pi] \times [-100, 100], \\ 0, & \text{otherwise.} \end{cases} \tag{15}$$

χ_B is the indicator function of the basin of attraction B and is given by

$$\chi_B = \begin{cases} 1, & \text{if } (\theta_m, \nu_m) \in B_m. \\ 0, & \text{otherwise.} \end{cases} \tag{16}$$

The basin of attraction B_m in our context is defined as

$$\begin{aligned} B_m = \{&(\theta_m(0), \nu_m(0)) \text{ where } \lim_{t\to+\infty} \theta_m(t) = \theta_m^S \text{ and } \lim_{t\to+\infty} \nu_m(t) = 0 : \\ &(\theta_n(0), \nu_n(0))_{n=1,\ldots,N} \in B \;\; \text{with} \;\; \theta_n(0) = \theta_n^S \;\; \text{and} \;\; \nu_n(0) = 0 \;\; \text{for all} \;\; n \neq m\}, \end{aligned} \tag{17}$$

which is a two-dimensional section of the 2N-dimensional synchronous state basin B.

The basin stability E_m express the chance of the system's component m to return to the synchronous state after a single node perturbation that occurs randomly with a probability density ρ. If $E_m = 0$, the synchronous state is unstable and if $E_m = 1$, the synchronous state is globally stable. In order to estimate E_m we use the Monte-Carlo method [25], where for each node, $T = 100$ initial states $(\theta_m(0), \nu_m(0))$ are chosen randomly according to ρ and their trajectories in phase space are calculated and the number U_m of times in which the system converges to the synchronous state is annotated. The other $N - 1$ nodes have a fixed initial condition $(\theta_n(0), \nu_n(0)) = (\theta_n^S, 0)$ for all $n \neq m$. The basin stability is then $E_m \approx \frac{U_m}{T}$ which has a standard error [12] of $e = \sqrt{\frac{E-E^2}{T}} \leq 5\%$.

3. Results and discussion

We use the Edge Snapping method by simultaneously integrating Eqs. (9) and (11) with a fixed coupling $\lambda = 1.5$ to generate a $N = 50$ node network whose delivered or consumed power ω are given by a Gaussian distribution with zero mean and standard deviation $\sigma_\omega = 0.2$ in a way that $\frac{N}{2}$ nodes have their frequencies set randomly by this distribution and $\frac{N}{2}$ nodes have the exact opposite frequency, so all the power generated is consumed and $\sum_{m=1}^{N} \omega_m = 0$. The topology of this network is plotted in Fig. 2 where in Fig. 2(a) the size of the nodes is proportional to their degree and the color relates to the amount of power ω delivered (red) or consumed (blue), while in Fig. 2(b) the probability of activation F is represented by edge colors, as the threshold for this configuration is $f^* = 0.56$, leaving the final topology with 108 edges. This is a relatively low number of edges as only a fraction of 0.08817 of all possible edges were marked as active in the final topology. It is a characteristics of the Edge snapping method to generate networks with a relatively low number of edges, which is an advantage when it comes to power grids due to the costs involved in the construction of transmission lines.

The degree of the nodes as a function of their power ω is plotted in Fig. 3(a). Let $|\omega_{mn}| = |\omega_m - \omega_n|$ be the absolute value of power difference between nodes m and n, in Fig. 3(b) the probability of activation of the edge connecting nodes m and n is plotted as a function of $|\omega_{mn}|$. The degree g of the nodes seem to be distributed mostly at random, as for the probability of activation F, it does not display a well defined behavior, although there is roughly a band-like structure and as $|\omega_{mn}|$ grows, the band structure gets narrower. The behavior of the degree and the probability of activation found

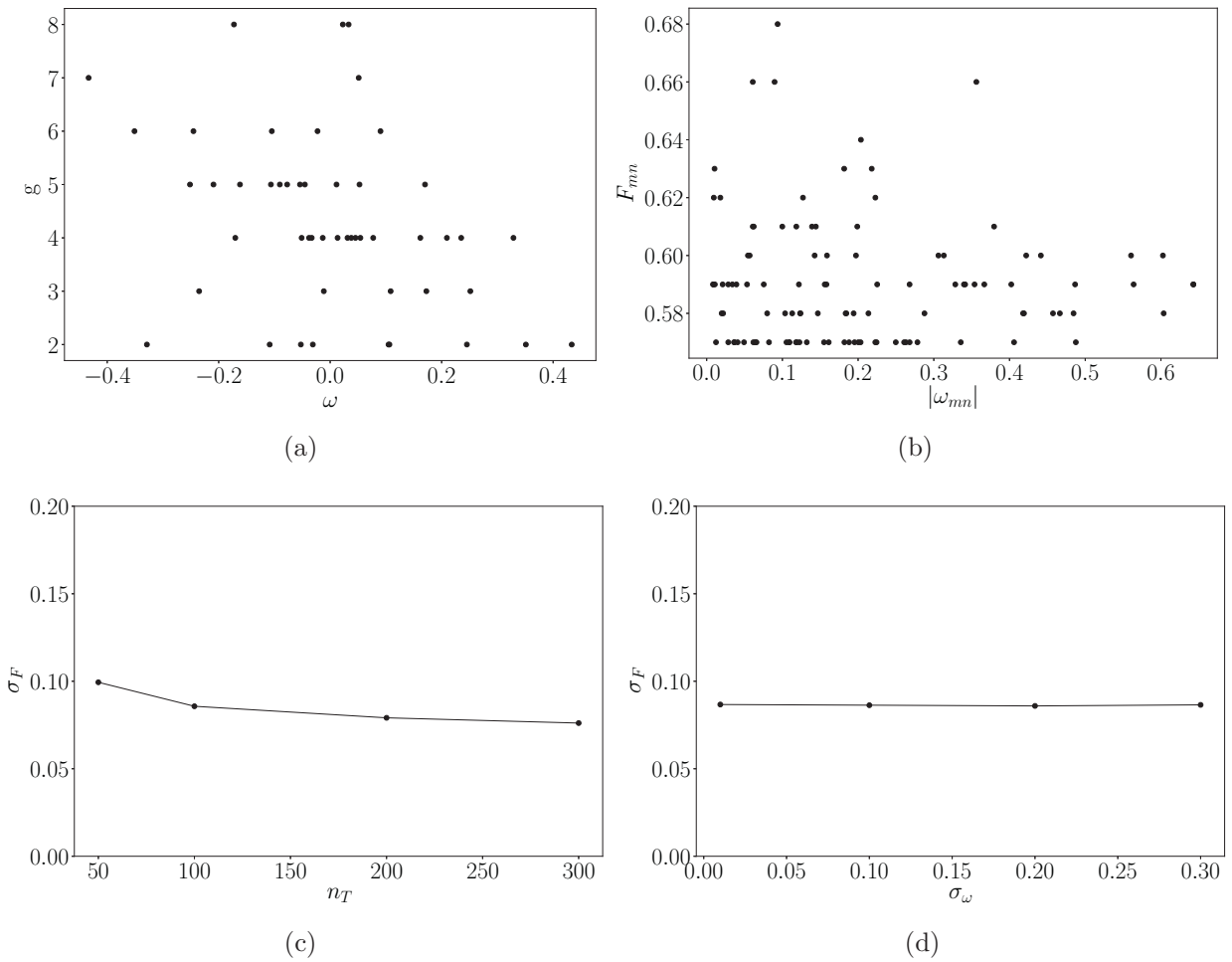

Fig. 3. (a) Node degree distribution as a function of the power ω. (b) Probability of activation F as a function of the power difference between nodes m and n. (c) Standard deviation of the matrix F as a function of the number of topologies n_T. (d) Standard deviation of F as a function of the standard deviation of the Gaussian distribution used to generate the power distribution ω.

here is the opposite of what was found in [15] by using the Edge Snapping method along with the first order Kuramoto model and, most importantly, the distribution of ω was given randomly by the same distribution used here but without the condition $\sum_{m=1}^{N} \omega_m = 0$. So, in [15], it is shown that the degree and the probability of activation are related to ω, in a way that the nodes with the value of ω far from the mean have higher degree and the probability of activation of the edges are greater for higher values of $|\omega_{mn}|$. We also obtained this behavior for both measures in our simulations for the second order Kuramoto model but when the condition $\sum_{m=1}^{N} \omega_m = 0$ is added to the distribution of power, this correlation seems to be lost. This condition is of utmost importance in this work as we are simulating a power grid in which all power generated is consumed.

Two parameters were fixed in our simulations, the standard deviation of the Gaussian distribution of ω, $\sigma_\omega = 0.2$, and the number of trials $n_T = 100$ used in the Evolutionary Edge Snapping, which gives the number of network topologies generated in order to calculate the matrix of the probability of activation F. The standard deviation of this matrix F as a function of the number of trials and as a function of the standard deviation of ω are plotted in Fig. 3(c) and (d), respectively. Note that σ_F does not vary much in both cases, so we consider the values of n_T and σ_ω we chose to be satisfactory.

Now that the network topology is defined, our interest is to study how it affects the synchronization of the power grid and in order to make some kind of comparison to see how efficient the ES network is, a random network with the same number nodes (50), edges (108) and with the same power distribution is generated, we name it Random network (since there is no consense when it comes to a network model that can fully represent a power grid topology, several researchers use the random model [26] to represent power grids as they both present exponential degree distribution [13,27]). Eq. (5) is integrated for both topologies, for several values of coupling λ in order to calculate the order parameter R and the partial synchronization index S. The initial conditions are fixed as $\theta_m(0) = 0.5$ and $\nu_m(0) = 0$ for $m = 1, \ldots, N$. The result can be seen in Fig. 4. The ES network reaches phase locking $S = 1$ at $\lambda = 0.60$ and the Random network reaches synchronization for

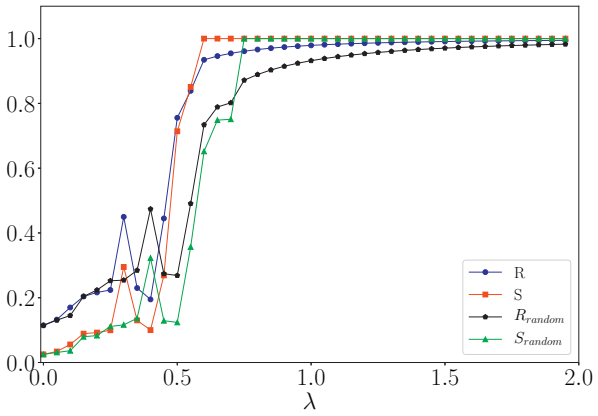

Fig. 4. Order parameter R (blue circle), partial synchronization index S (red square) of the ES network and order parameter (black hexagon) and partial synchronization index (green triangle) of the Random network as a function of the maximum power transmission capacity λ. (For interpretation of the references to color in this figure legend, the reader is referred to the web version of this article.)

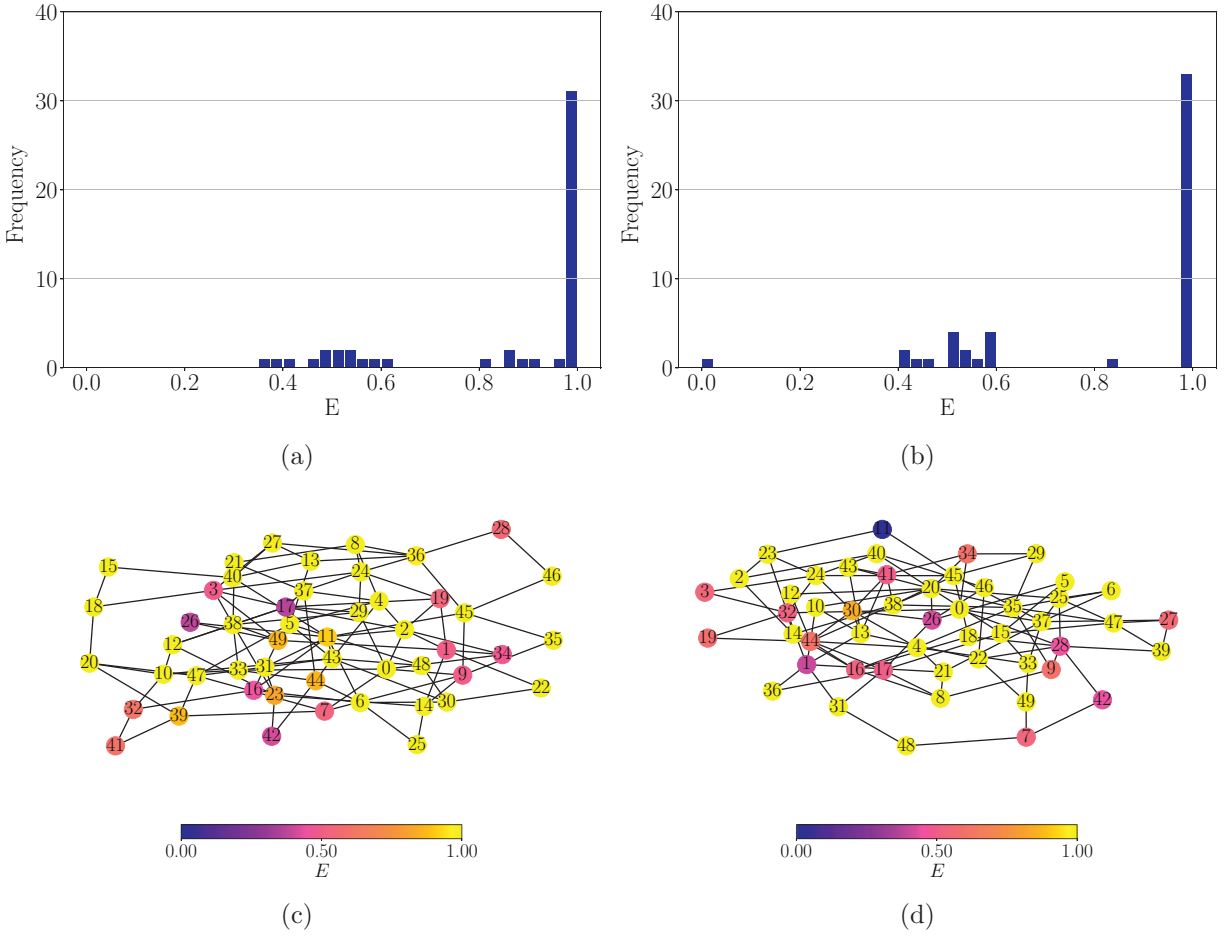

Fig. 5. Histogram of the basin stability for the (a) ES network and for the (b) Random network. Basin stability of each node for the (c) ES and (d) Random networks.

$\lambda = 0.75$. Note that for higher values of coupling the value of the order parameter R is close but never equal to one, which is expected because, as mentioned in Section 2.1, it is a condition to have a power flow between two nodes of a power grid. The advantage of reaching synchronization at lower values of coupling comes from the fact that the coupling represents the maximum power transfer capacity of a transmission line and, therefore, lower transfer capacity means lower voltage levels and cheaper transmission lines when building power grids.

In order to study the stability of the ES network topology we use the basin stability method presented in Section 2.3, where at a fixed value of coupling ($\lambda = 1.5$) a single node m suffers a perturbation $T = 100$ times. Let U_m be the number of times the system reaches synchronization, then the basin stability of node m is approximately $E_m = \frac{U_m}{T}$. The same is done for the Random network. The histogram and the value of the basin stability of each node for both networks and can be seen in Fig. 5. Note that for the ES network, 74% of the nodes present a relatively high stability, that is, $E \geq 0.8$, as for the Random network, this value drops to 68%.

4. Conclusions

In this paper, we used the Edge Snapping method to generate power grids whose generator and consumers are modeled by the second order Kuramoto oscillator model. A fifty node power grid was generated, being that half of the nodes were set to be consumers and the other half generators in a way that all power produced is consumed by the grid. The topologies generated by the Edge Snapping method have a characteristic of having a relatively low number of nodes, which is desirable in our case study since it means building less transmission lines. Also, the network generated by this method favors synchronization in a way that it reaches phase locking at a lower value of coupling when compared to a random network with the same number of nodes and edges. As the coupling in the second order Kuramoto model is related to the maximum transmission capacity of a transmission line, lower coupling implies lower voltage levels in the transmission lines which is also a desirable characteristics in a power grid. The ES network presented a higher number of stable nodes when compared to the random network of the same size.

Acknowledgments

Juliana C. Lacerda and Jussara Dias would like to thank Conselho Nacional de Desenvolvimento Científico e Tecnológico – CNPq for the financial support. This research is also supported by grant 2015/50122-0 of São Paulo Research Foundation (FAPESP) and DFG-IRTG 1740/2.

References

[1] Y. Koç, M. Warnier, R.E. Kooij, F.M. Brazier, An entropy-based metric to quantify the robustness of power grids against cascading failures, Saf. Sci. 59 (2013) 126–134.
[2] J. Grzybowski, E.E. Macau, T. Yoneyama, Power-grids as complex networks: emerging investigations into robustness and stability, in: Chaotic, Fractional, and Complex Dynamics: New Insights and Perspectives, Springer, 2018, pp. 287–315.
[3] H. Haes Alhelou, M.E. Hamedani-Golshan, T.C. Njenda, P. Siano, A survey on power system blackout and cascading events: Research motivations and challenges, Energies 12 (4) (2019) 682.
[4] M. Panteli, P. Mancarella, Influence of extreme weather and climate change on the resilience of power systems: Impacts and possible mitigation strategies, Electr. Power Syst. Res. 127 (2015) 259–270.
[5] D.M. Ward, The effect of weather on grid systems and the reliability of electricity supply, Clim. Change 121 (1) (2013) 103–113.
[6] D. Infield, L. Freris, Renewable Energy in Power Systems, John Wiley & Sons, 2020.
[7] P. Piagi, R.H. Lasseter, Autonomous control of microgrids, in: Proceedings of the 2006 IEEE Power Engineering Society General Meeting, 2006, p. 8.
[8] L. Zhu, D.J. Hill, Synchronization of Power Systems and Kuramoto Oscillators: A Regional Stability Framework, arXiv preprint arXiv:1804.01644 (2018).
[9] J. Grzybowski, E. Macau, T. Yoneyama, On synchronization in power-grids modelled as networks of second-order Kuramoto oscillators, Chaos: Interdiscip. J. Nonlinear Sci. 26 (11) (2016) 113113.
[10] S.H. Strogatz, Nonlinear Dynamics and Chaos, Westview Press, Boulder, 2014.
[11] G. Filatrella, A.H. Nielsen, N.F. Pedersen, Analysis of a power grid using a Kuramoto-like model, Eur. Phys. J. B 61 (4) (2008) 485–491.
[12] P.J. Menck, J. Heitzig, N. Marwan, J. Kurths, How basin stability complements the linear-stability paradigm, Nat. Phys. 9 (2) (2013) 89.
[13] P.J. Menck, J. Heitzig, J. Kurths, H.J. Schellnhuber, How dead ends undermine power grid stability, Nat. Commun. 5 (2014) 3969.
[14] P. DeLellis, F. Garofalo, M. Porfiri, et al., Evolution of complex networks via edge snapping, IEEE Trans. Circuits Syst. I: Regul. Pap. 57 (8) (2010) 2132–2143.
[15] F. Scafuti, T. Aoki, M. di Bernardo, Heterogeneity induces emergent functional networks for synchronization, Phys. Rev. E 91 (6) (2015) 062913.
[16] P. Kundur, N.J. Balu, M.G. Lauby, Power System Stability and Control, 7, McGraw-Hill New York, 1994.
[17] A. Monticelli, A. Garcia, Introdução a Sistemas de Energia Elétrica, Editora UNICAMP, 2011.
[18] B.C. Daniels, Synchronization of Globally Coupled Nonlinear Oscillators: The Rich Behavior of the Kuramoto Model, Ohio Wesleyan Physics Dept., Essayvol. 7(2) (2005).
[19] J. Gómez-Gardenes, Y. Moreno, A. Arenas, Paths to synchronization on complex networks, Phys. Rev. Lett. 98 (3) (2007) 034101.
[20] J.C. Lacerda, C. Freitas, E.E. Macau, Symbolic dynamical characterization for multistability in remote synchronization phenomena, Front. Appl. Math. Stat. 6 (2020) 15.
[21] J. Lacerda, C. Freitas, E. Macau, Multistable remote synchronization in a star-like network of non-identical oscillators, Appl. Math. Model. 69 (2019) 453–465.
[22] G. Ódor, B. Hartmann, Heterogeneity effects in power grid network models, Phys. Rev. E 98 (2) (2018) 022305.
[23] M. Rohden, A. Sorge, M. Timme, D. Witthaut, Self-organized synchronization in decentralized power grids, Phys. Rev. Lett. 109 (6) (2012) 064101.

[24] F. Scafuti, T. Aoki, M. di Bernardo, An evolutionary strategy for adaptive network control and synchronization and its applications, IFAC-PapersOnLine 48 (18) (2015) 193–198.
[25] D.A. Wiley, S.H. Strogatz, M. Girvan, The size of the sync basin, Chaos: Interdiscip. J. Nonlinear Sci. 16 (1) (2006) 015103.
[26] P. Erdös, A. Rényi, On random graphs, I, Publ. Math. (Debrecen) 6 (1959) 290–297.
[27] P. Hines, S. Blumsack, E.C. Sanchez, C. Barrows, The topological and electrical structure of power grids, in: Proceedings of the 43rd Hawaii International Conference on System Sciences, IEEE, 2010, pp. 1–10.